

Discrete Talbot Effect

Robert Iwanow, Daniel May-Arrijoja, Demetrios N. Christodoulides, George I. Stegeman, Yoohong Min and Wolfgang Sohler

The repeated self-imaging of a diffraction grating—a classical effect in optics—was first reported by Talbot in 1836.¹ Lord Rayleigh explained this remarkable phenomenon a few decades later when he showed that any periodic one-dimensional field pattern reappears, upon propagation, at even integer multiples of the so-called Talbot distance $z_T = D^2/\lambda$, where D represents the spatial period of the pattern and λ is the light wavelength. In addition to the integer Talbot effect, fractional as well as fractal revivals are also known to occur at distances that are rational or irrational multiples of z_T , respectively.²

Lately, the optical research community has shown considerable interest in wave propagation phenomena in discrete structures. Arrays or lattices of evanescently coupled waveguides or chains of coupled microresonators are prime examples of structures where discrete optical wave dynamics can be observed.³ One question that has naturally arisen is whether the Talbot effect is also possible in discrete systems.

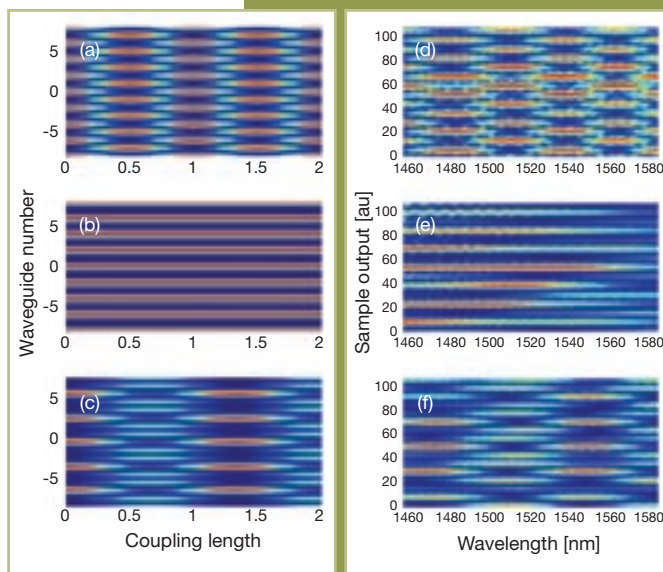
We have recently reported the first experimental observation of discrete Talbot effects in weakly coupled waveguide arrays.⁴ We found that, unlike in continuous systems where the Talbot self-imaging effect always occurs irrespective of the pattern period, in discrete configurations this process is only possible for a specific set of periodicities N . In discrete structures, the periodicities leading to discrete Talbot revivals are those for which the cosine of $\cos(2\pi/N)$ is a rational number. This is only possible when the period N of the initial pattern belongs to the set $\{1, 2, 3, 4, 6\}$.

The left column of the figure depicts the theoretically anticipated Talbot

intensity patterns (as viewed from the top) as a function of propagation distance or coupling length when the waveguide array is excited with a spatially periodic input. Parts (a), (b) and (c) were obtained using a $\{1, 0, 1, 0, \dots\}$, $\{1, 0, -1, 0, \dots\}$ and a $\{1, 0, 0, 1, 0, 0, \dots\}$ periodic input, respectively. In all cases, a “carpet” appears—in other words, the input pattern repeats periodically.

The absence of any revivals in (b) is due to the fact that the $\{1, 0, -1, 0, \dots\}$ pattern excites the lattice at the middle of the Brillouin zone (at $\pi/2$), where the effective diffraction of the array is zero,⁵ and so the Talbot process that derives from this effect vanishes. To demonstrate discrete Talbot effects, we used a channel waveguide array consisting of 101 guides, fabricated on 70-mm-long Z-cut LiNbO₃. Because of the sample's excellent linear properties (low scattering), we were not able to observe the Talbot revivals when looking from the top.

Instead, indirect observation of the Talbot process at the output of the array was possible. We accomplished this by varying the wavelength (and hence the coupling length) over the full spectral range of the probing semiconductor laser (1456 to 1584 nm). This change in coupling strength with wavelength is essentially equivalent to varying the effective sample length. Amplitude masks were also used to excite the array with a periodic input. The experimental results corresponding to the excitation conditions simulated in (a), (b) and (c) are shown in (d), (e) and (f). In these figures, the intensity



Talbot intensity “carpets” as a function of propagation distance for different periodic input field patterns: (a) $\{1, 0, 1, 0, \dots\}$, (b) $\{1, 0, -1, 0, \dots\}$, (c) $\{1, 0, 0, 1, 0, 0, \dots\}$. Experimental results corresponding to the excitation conditions simulated in (a), (b) and (c) are shown in (d), (e) and (f). In the latter set of figures, the intensity at the output of the array is shown as a function of wavelength.

at the output of the array is shown as a function of wavelength. The experimental results agreed well with theory.

In conclusion, we have observed for the first time discrete Talbot revivals in waveguide arrays. Unlike continuous systems, where the Talbot self-imaging effect always occurs irrespective of the pattern period, in discrete configurations this process is only possible for a specific set of periodicities. \blacktriangle

[Robert Iwanow, Daniel May-Arrijoja, Demetrios N. Christodoulides and George I. Stegeman are with the College of Optics and Photonics, CREOL & FPCE, University of Central Florida, Orlando, Fla. Yoohong Min and Wolfgang Sohler are from the University of Paderborn, Paderborn, Germany.]

References

1. H.F. Talbot, *Philos. Mag.* **9**, 401 (1836).
2. M.V. Berry and S. Klein, *J. Mod. Opt.* **43**, 2139 (1996).
3. D.N. Christodoulides et al., *Nature* **424**, 817 (2003).
4. R. Iwanow et al., *Phys. Rev. Lett.* **95**, 053902 (2005).
5. H.S. Eisenberg et al., *Phys. Rev. Lett.* **85**, 1863 (2000).

Lidar Measurements of Honey Bees for Locating Land Mines

Joseph A. Shaw, Nathan L. Seldomridge, Dustin L. Dunkle, Paul W. Nugent, Lee H. Spangler, Jerry J. Bromenshenk, Colin B. Henderson, James H. Churnside and James J. Wilson

We have demonstrated the use of scanning lidar (light detection and ranging) for measuring honey bee density to locate buried land mines.¹ The bees are conditioned through feeding to seek out the odor of explosives, which leads them to pause in the vicinity of a mine.² The backscattered lidar signal is used to produce spatial maps of bee density that indicate the location of the explosives (bees spend more time in the vicinity of chemical plumes emanating from the mines).¹

In July and August 2003, we conducted an experiment to demonstrate

the utility of lidar for generating the bee density measurements required to make practical use of the bees as mine detectors. We conducted this blind experiment at a live mine field (with unfused mines) at Fort Leonard Wood, Mo. We used a direct-detection lidar system based on a pulsed, frequency-doubled Nd:Yag laser (532-nm wavelength, 10-ns pulsewidth, 100 mJ pulse energy).

The lidar receiver collected light through a linear polarizer and 17.5-cm-diameter refractive telescope onto a detector, whose signal was logarithmically amplified and digitized at a rate of 1 G sample/s with 8-bit resolution. The lidar scanned the entire minefield once each 13 s from a distance of 83 m.

The figure is a plot of the lidar signal obtained from a single scan across the mine field, with cross-scan distance on the abscissa (x), range on the ordinate (y) and signal strength on the z axis. Large spikes occur where the lidar beam intersects obstructions, such as corner posts and camera tripods located in the mine field for independent validation of bee density, and the smaller spikes are bees.

This experiment showed that bees were best detected with a co-polarized lidar and that the lidar reliably detected regions of higher bee density correlated with locations of high chemical plume density determined with *in situ* chemical sampling. Real-time observations of the lidar data even led to the discovery of a previously unknown explosive plume

inside a control region that was supposedly free of explosives.

We characterized the bee scattering by determining the scattering cross-section and depolarization ratio in field measurements and by measuring the depolarization ratio of bee bodies and wings in the laboratory. The field measurements yielded a mean scattering cross-section of 0.093 cm² and depolarization ratio of 0.39 ± 0.1, while the laboratory measurements yielded a depolarization ratio of approximately 0.15–0.30 for bee bodies and 0–0.1 for bee wings.

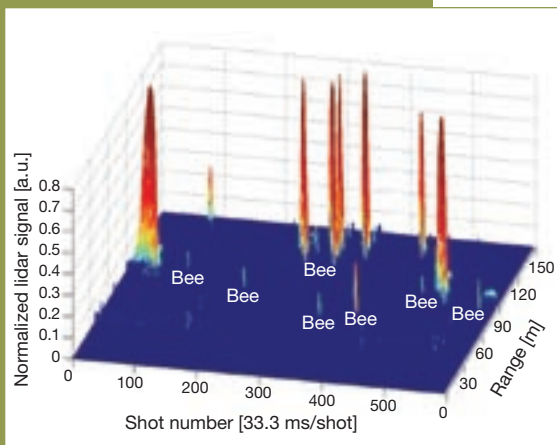
While the results of the field experiment were positive and highly encouraging, it was difficult, or nearly impossible, to distinguish between bees and vegetation or other obstructions in the direct-detection lidar signal. Consequently, our present and future research will focus on the development and use of laser sensors that detect bees with a more bee-specific signature. ▲

The same authors published a summary of work, which can be found under the title, "Polarization lidar measurements of honey bees in flight for locating land mines." It is available in Opt. Express 13 (15), 5853-63 (2005), or <http://www.opticsexpress.org/abstract.cfm?URI=OPEX-13-15-5853>.

[J.A. Shaw, N.L. Seldomridge, D.L. Dunkle and P.W. Nugent are with the Electrical and Computer Engineering Department, Montana State University, Bozeman, Mont. L.H. Spangler is with the Chemistry and Biochemistry Department, also at Montana State University. J.J. Bromenshenk and C.B. Henderson are with the Division of Biological Sciences, University of Montana, Missoula, Mont. J.H. Churnside and J.J. Wilson are with the NOAA Environmental Technology Laboratory, Boulder, Colo.]

References

1. J.A. Shaw et al. *Opt. Express* **13** (15), 5853-63 (2005).
2. J.J. Bromenshenk et al. *J. Mine Action* **7.3** (2003), maic.jmu.edu/journal/7.3/focus/bromenshenk/bromenshenk.htm.



Partially processed lidar data for a single 13-s scan across the mine field. Large spikes occur where the lidar beam intersects obstructions, such as corner posts and camera tripods located in the mine field for independent validation of bee density, and the smaller spikes are bees.